Laser cooling of stored bunched relativistic Li-like oxygen ions

W. Q. Wen [1,2,*] H. B. Wang [1,2] D. Y. Chen,[1,2] Z. K. Huang,[1,2] Y. J. Yuan [1,2] D. C. Zhang [3] D. Winters [4]
S. Klammes [4] S. Litvinov [4] D. Kiefer,[5] Th. Walther [5,6] M. Loeser [7] M. Siebold,[7] U. Schramm,[7,8] N. Khan,[1] J. Li [1]
M. T. Tang,[1] J. X. Wu,[1] D. Y. Yin,[1] L. J. Mao,[1] J. C. Yang,[1] S. F. Zhang,[1,2] M. Bussmann,[7,9] and X. Ma [1,2,†]

[1]*Institute of Modern Physics*, Chinese Academy of Sciences, 730000, Lanzhou, China
[2]*University of Chinese Academy of Sciences*, 100049, Beijing, China
[3]*School of Optoelectronic Engineering, Xidian University, 710071, Xi'an, China*
[4]*GSI Helmholtzzentrum für Schwerionenforschung GmbH*, D-64291 Darmstadt, Germany
[5]*Institut für Angewandte Physik, Technische Universität Darmstadt, 64289 Darmstadt, Germany*
[6]*Helmholtz Research Academy Hesse for FAIR, Campus Darmstadt, 64289 Darmstadt, Germany*
[7]*Helmholtz-Zentrum Dresden-Rossendorf, Bautzner Landstrasse 400, 01328 Dresden, Germany*
[8]*Technische Universität Dresden, 01069 Dresden, Germany*
[9]*Center for Advanced Systems Understanding, 02826 Görlitz, Germany*

We report the experimental demonstration of laser cooling of bunched Li-like $^{16}O^{5+}$ ion beams at $\sim$64% of the speed of light in the storage ring CSRe. The longitudinal dynamics of laser-cooled bunched ion beams were investigated by observing the Schottky signals in real time with a high-sensitivity Schottky resonator. Furthermore, a multiparticle phase-space tracking code was developed to simulate the longitudinal Schottky spectrum of the ions inside the bucket and to interpret the experimental observations and derive the momentum distribution of the laser-cooled beams. We demonstrate that the relative longitudinal momentum spread of O^{5+} ion beams reached $\Delta p/p \approx 2.0 \times 10^{-6}$ with laser cooling, which is one order of magnitude smaller than what can be reached by electron cooling. The laser-cooling technique and the simulation method developed in this work can be applied to study phase-transition effects of bunched ion beams at storage rings and also pave the way for laser-cooling and precision laser spectroscopy experiments at the future large heavy-ion accelerator facilities HIAF (China) and FAIR (Germany), and the proposed Gamma Factory at CERN.

Laser cooling and manipulation of ions in traps has proven to be extremely powerful and valuable for atomic physics, precision metrology, and fundamental symmetries studies [1–5]. In addition, laser cooling is considered to be the most promising method to realize the phase transition from the intrabeam scattering regime to the space-charged dominated and even crystalline ion-beam regime at storage rings, which are of great interest for accelerator physics and precision measurements in atomic physics and nuclear physics [6–10]. Laser cooling of stored coasting Li^+ ion beams was first demonstrated at the storage rings TSR and ASTRID, and ultracold ion beams with a temperature of only a few kelvin [11] down to $\sim$millikelvin [12] have been realized. In order to counteract the laser force, the technique of bunched-beam laser cooling has been developed and demonstrated with Mg^+ [13] and Be^+ [14] ion beams by using only one laser beam together with a radio-frequency (rf) buncher. Later, laser cooling of bunched relativistic C^{3+} ion beams was realized at the storage ring ESR at GSI [15]. In these experiments, Schottky signals were employed to diagnose the longitudinal dynamics of the cooled ion beams. However, it is still not fully understood how to

properly diagnose the longitudinal dynamics from intrabeam scattering to space-charge dominated regimes [16,17] and how to derive the momentum spread of laser-cooled bunched ion beams from the Schottky spectrum [18,19].

As of today, only a few ion species have been laser cooled at heavy-ion storage rings due to the very short transition wavelengths in highly charged ions (HCIs) and the lack of suitable laser systems at those wavelengths [7]. Since the laser-cooling force on relativistic ion beams scales approximately with γ^2 (relativistic Lorentz factor γ), the time required to cool down an ion beam with a broad initial momentum spread by a broadband laser is of the order of seconds [20,21]. This is very short as compared to other ion-beam cooling techniques, such as electron cooling [22] and stochastic cooling [23]. In addition to laser cooling at storage rings, precision laser spectroscopy experiments of HCIs can be performed simultaneously to test quantum electrodynamics (QED) effects [24,25]. This strongly motivates further experimental and theoretical investigations. Therefore, laser cooling and precision laser spectroscopy of relativistic HCIs are among the significant topics for the High Intensity heavy-ion Accelerator Facility (HIAF) in Huizhou, China [26,27] and the Facility for Antiproton and Ion Research (FAIR) in Darmstadt, Germany [28]. Very recently, laser excitation of extremely relativistic ($\gamma \approx 100$) bunched heavy-ion beams at the Super Proton Synchrotron (SPS) was proposed as a

*Contact author: wenweiqiang@impcas.ac.cn
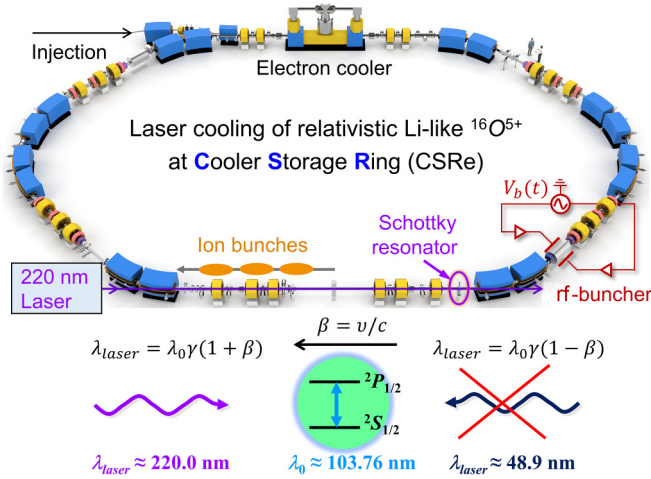†Contact author: x.ma@impcas.ac.cn

FIG. 1. Schematic of the laser cooling setup at the CSRe. A counterpropagating cw UV laser beam was overlapped with the ion beam in the straight section. The rf buncher was used to bunch the ion beams and the Schottky resonator was used to monitor the dynamics of the cooling process.
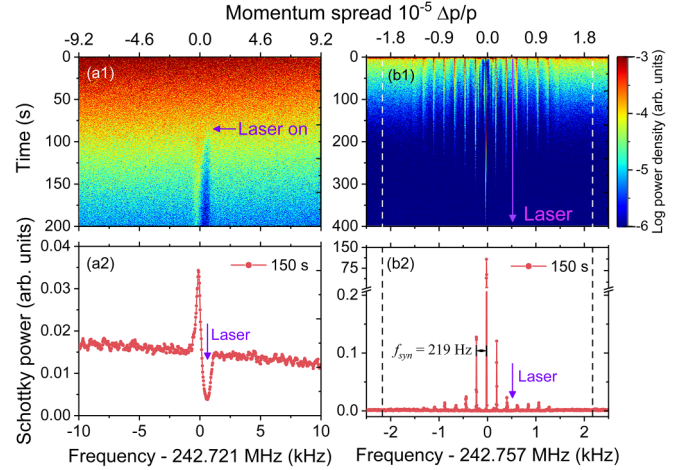

FIG. 2. Schottky spectra of stored relativistic O^{5+} ions interacting with a fixed-frequency cw laser (purple arrow) in the CSRe. (Upper row) Schottky signal vs time for (a1) a coasting ion beam and (b1) a bunched ion beam. The intensity of the Schottky power density is color coded logarithmically. (Lower row) Projection of the Schottky spectrum at 150 s after injection for (a2) a coasting ion beam and (b2) a bunched ion beam. The acceptance of the rf bucket is indicated by the distance between the two dashed lines in (b1) and (b2).

proof-of-principle experiment for the Gamma Factory at CERN [29–31].

In this Letter, we present the results of laser cooling of bunched $^{16}O^{5+}$ ion beams at relativistic energy at the CSRe at Heavy-Ion Research Facility in Lanzhou (HIRFL) [32]. A schematic view of the laser-cooling setup at the CSRe is shown in Fig. 1. Li-like oxygen ions were injected and stored in the CSRe with a kinetic energy of 275.7 MeV/u, which corresponds to a velocity of 63.6% of the speed of light c. Given the circumference of the CSRe of 128.8 m, the revolution frequency of the O^{5+} ion was $f_{\text{rev}} = 1.48$ MHz. A dc current transformer was used to measure the ion-beam current, and the number of stored O^{5+} ions after injection was about 10^8. The residual gas pressure in the storage ring was 5×10^{-11} mbar, yielding the lifetime of the stored ion beam of about 35 s. A Schottky resonator [33,34], which worked at a frequency of about 243 MHz, was employed to continuously measure the revolution frequency and the longitudinal momentum spread ($\Delta p/p$) of the ion beams. For the uncorrelated motion of the ions in the beam, the relative revolution frequency spread ($\Delta f/f$) and the integrated Schottky signal power were proportional to $\Delta p/p$ and the number of stored ions (N), respectively [35,36]. The momentum spread measured at the first harmonic of the revolution frequency can be written as $\frac{\Delta p}{p} = \eta^{-1} \frac{\Delta f_{\text{rev}}}{f_{\text{rev}}}$, where $\eta = 0.45$ is the phase-slip factor at the CSRe.

In the frame of the relativistic moving O^{5+} ions, as shown in Fig. 1, the wavelength of the laser (λ_{laser}) will appear strongly Doppler shifted ("Lorentz boost"). The relation between λ_{laser} and the transition wavelength in the ion rest frame (λ_0) is

$$\lambda_{\text{laser}} = \lambda_0 \gamma (1 - \beta \cos \theta). \tag{1}$$

Here, θ is the angle between the directions of the laser beam and the ion beam, $\gamma = 1/\sqrt{1 - \beta^2}$, and $\beta = \upsilon/c$ the velocity of the ions. To match the wavelength ($\lambda_0 = 103.76$ nm) of

the closed $1s^2 2s^2 S_{1/2} \rightarrow 1s^2 2p^2 P_{1/2}$ transition in O^{5+}, the laser wavelength must be $\lambda_{\text{laser}} = 220$ nm for counterpropagating and $\lambda_{\text{laser}} = 48.9$ nm for copropagating directions (not available), respectively. In the present experiment, a single counterpropagating 220-nm laser beam was employed to resonantly excite the $2s - 2p$ transition of O^{5+} ions with natural linewidth $\Gamma \approx 65$ MHz. The ion beam was overlapped with the laser beam over a distance of 25 m along one straight section of the CSRe. The overlap was optimized using scrapers with a precision better than 1 mm. A Toptica TA-FHG pro laser system was employed to generate the 220-nm cw radiation with a linewidth of 200 kHz and a power of about 30 mW, and focus the ultraviolet light onto a 1-mm^2 spot in the center of the interaction section.

We have moderately bunched the ion beams to provide the position-dependent friction bucket force for counteracting the laser-cooling force, i.e., bunching frequency $f_b = hf_{\text{rev}} = h\upsilon/C$, where C is the circumference of the CSRe. The harmonic number $h = 33$ determines the number of ion bunches in the storage ring. By passing the rf buncher, the ions experience a longitudinal modulation force, called the rf bucket force. The ions captured inside the rf bucket will perform slow synchrotron oscillations around the synchronous ion. cw laser cooling of bunched ion beams relies on the damping the synchrotron oscillation amplitude by the resonant laser force [13,37], the detailed description of the methods and derivations are shown in the Appendix.

The first step to perform laser cooling of bunched O^{5+} ion beams at the CSRe is to find the energy resonance as described by Eq. (1). The resonant interaction between the laser and ion beams was observed in a longitudinal Schottky spectrum with the laser switched on 80 s after beam injection, as shown in Fig. 2(a1). Figure 2(a2) is the projection of the
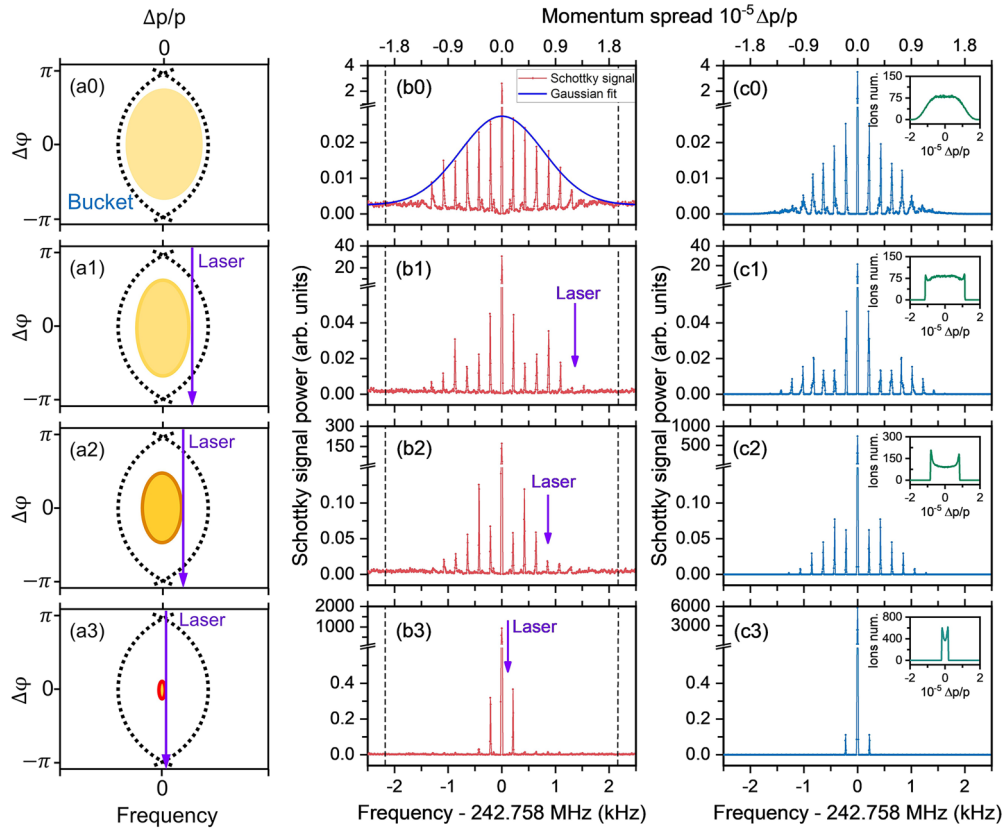
FIG. 3. (Left row) Schematic evolution of phase space for bunched O^{5+} ions inside the rf bucket without (a0) and with (a1)–(a3) laser cooling. The corresponding experimental and simulated Schottky spectra are shown in (Middle row) (b0)–(b3) and (Right row) (c0)–(c3), respectively. The positions of the laser are marked by the solid purple arrow. The detuning Δf_b is gradually reduced from (a1) to (a3), and the ion beams clearly "cool down" (smaller width), which can be seen from the corresponding measured (b1)–(b3) and simulated (c1)–(c3) Schottky spectra. The insets in (c0)–(c3) show the momentum distributions of the ion beams used in the simulation.

Schottky intensity of Fig. 2(a1) onto the frequency axis at 150 s after injection. The strong dip implies that all ions with this particular velocity class have interacted with the laser and were decelerated, as indicated by the pileup at a slightly lower frequency (ion velocity). Once the cooling transition was found, we bunched the O^{5+} ion beam and performed the laser-cooling experiment by a slight red detuning of the laser wavelength to the center of the rf bucket, as shown in Fig. 2(b1). The projection of a cut at 150 s after injection is shown in Fig. 2(b2), and the estimated number of ions inside the rf bucket is $\sim 1 \times 10^5$. It can be seen that the Schottky spectrum of a bunched laser-cooled ion beam shows sharp and pronounced peaks with equidistant spacing given by the synchrotron frequency of the ions in the rf bucket. The central peak marks the center of the bunch in frequency space. The "effective" bunching voltage and the full acceptance of the rf bucket in momentum space are $U_b = 14.5$ V and $\Delta p/p \approx 4.0 \times 10^{-5}$, respectively, which are deduced from $f_{\text{syn}} \approx 219$ Hz [38].

In order to fully interpret the experimental observations, a multiparticle phase-space tracking method, based on a differential equation model, has been developed to simulate the longitudinal Schottky spectra of laser-cooled bunched ion beams. The parameters of the storage ring and the ion beam, i.e., the machine settings and the phase-space redistribution, are the input for the code. The evolution of the ions in phase space

is then computed by a linear transfer matrix, turn by turn. Then, the ion changes its average longitudinal and transverse momentum by absorption and emission of a photon in the laboratory reference frame. Finally, the Schottky spectrum can be obtained by performing a fast Fourier transform of the simulated Schottky signals. In the simulation, the number of particles inside the rf bucket is set to 1.5×10^4, and the number of laser-ion interaction revolution cycles is set to 2^{18} turns. Since the density of the ions inside the rf bucket is very low, the intrabeam scattering (IBS) as well as the space-charge effects are neglected in the simulation. Thus, it is assumed that the ions oscillate independently in a harmonic rf bucket potential. The details of the simulation method have been described in Refs. [39,40].

First, we compare the Schottky spectrum of a bunched ion beam with the simulation as shown in Figs. 3(b0) and 3(c0) without laser interaction. The phase space of the ions inside the rf bucket is shown in Fig. 3(a0). A Gaussian distribution was used to estimate the longitudinal momentum spread of the ions in the rf bucket as discussed in Refs. [15,16], an example is shown in Fig. 3(b0), where 1σ of $\Delta p/p \approx 7.1 \times 10^{-6}$ was obtained. The simulations were performed using a Rice distribution of the synchrotron amplitude [41]. The corresponding initial momentum distribution, which is used for all simulations, is shown in the inset of Fig. 3(c0) and has a rms momentum spread of $\Delta p/p \approx 7.2 \times 10^{-6}$. The simulated

Schottky spectrum agrees very well with the experimental one. The simulation also demonstrates that the very strong central line comes from the coherent motion of the ions inside the rf bucket and the sidebands originate from the incoherent ion motion. These amplitudes add incoherently due to the random phases of the synchrotron oscillations. Therefore, the rms momentum spread of the bunched beam can be obtained by using the Schottky sideband distribution without taking into account the central line, as proposed in Ref. [42], and shown with more details in the Appendix. The thus-determined rms momentum spread from the experimental Schottky spectrum is $\Delta p/p \approx 7.5 \times 10^{-6}$. This, in turn, agrees very well with the rms spread of the distribution used for the simulation.

Systematic investigations of longitudinal dynamics of the laser-cooled bunched ion beams are shown in Figs. 3(a1)–3(c3), and the experimental Schottky spectra are the projection of the Schottky power density onto the frequency axis at 150 s after injection. The laser has been fixed by detuning of bunching frequency in all of the measurements, and the detuning (Δf_b) was done by varying the bunching frequency. It can be found clearly that the width of the Schottky sideband distribution is shrinking and therefore the momentum spread of the ion beam also decreases continuously as the center of the rf bucket approaches the laser position, as indicated by the arrows in Figs. 3(a1)–3(a3) and 3(b1)–3(b3).

In Fig. 3(a1) the separatrix [13] of the rf bucket is close to the fixed laser position, and only ions with momentum close to the bucket acceptance will be in resonance and thus be decelerated by the laser, indicated by the arrow as shown in the experimental Schottky spectrum of Fig. 3(b1). The sidebands close to the laser position are stronger than in Fig. 3(b0), indicating that the laser-cooled ions are accumulated at this velocity range. This is also confirmed by the simulation, shown in Fig. 3(c1). In this case, the longitudinal momentum spread of the laser-cooled ions can only be derived from the rms of the incoherent sidebands of the Schottky spectrum, and the deduced experimental and simulated rms are $\Delta p/p \approx 6.5 \times 10^{-6}$ and $\Delta p/p \approx 6.4 \times 10^{-6}$, respectively.

In Fig. 3(a2) the detuning Δf_b is reduced, and as a result, ions with smaller oscillation amplitudes come into resonance with the laser. Synchrotron oscillations with larger amplitudes are damped until these ions are cooled below the laser position, as shown in Fig. 3(b2), which agrees with the simulation shown in Fig. 3(c2). This indicates that the cooling dynamics can be reasonably well simulated and understood, even though IBS and space-charge effects are not considered. In this case, the experimental rms momentum spread of laser-cooled ion beams corresponds to $\Delta p/p \approx 5.1 \times 10^{-6}$.

In Fig. 3(a3), the detuning almost reaches its minimum value and the center of the rf bucket is very close to the laser position. From Fig. 3(b3) it can be seen that the Schottky spectrum becomes very narrow with only one sideband appearing on each side of the strong coherent central peak and therefore almost all ions are cooled to the center of the rf bucket. Figure 3(c3) shows that the simulated Schottky spectrum has a similar shape but with a much stronger central peak and lower sidebands as compared to the experiment. A determination of the rms momentum spread $\Delta p/p \approx 2 \times 10^{-6}$, as given by the width of the Schottky spectrum, reaches its resolution.
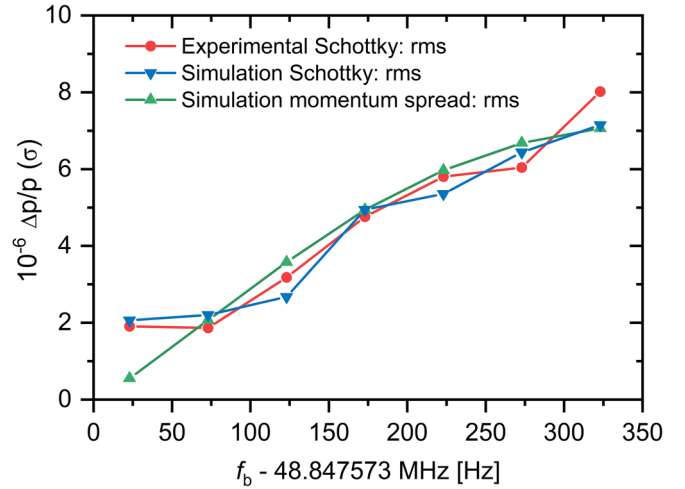

FIG. 4. Longitudinal rms momentum spread plotted as a function of the bucket detuning Δf_b relative to the laser position.

The rms values of the relative momentum spread, derived from the experimental and simulated incoherent Schottky sidebands, as well as the input momentum distribution of the simulation, are shown in Fig. 4. They agree well with each other, except at the very small detuning frequency. The rms momentum spread from the Schottky spectrum reaches a minimum of $\Delta p/p \approx 2 \times 10^{-6}$ and levels off when the detuning frequency is less than about 0.1 kHz. At this point, the laser-cooled ion beams with very low temperature will approach the space-charge dominated regime, the estimated plasma coupling parameter $\Gamma_P = \frac{Q_e^2}{4\pi\varepsilon_0 a_{WS} k_B T}$ is around 0.03, which is between the emittance-dominated regime ($\Gamma_P \ll 1$) and the space-charge dominated regime ($\Gamma_P \approx 1$). As a result, the IBS scattering rates are still very low and the longitudinal ion dynamics can be modeled by neglecting the ion-ion Coulomb interaction [43–45]. Since the determination of the momentum spread requires the existence of at least one sideband on each side of the central peak in the Schottky spectrum, a precise derivation of the very small $\Delta p/p$ of laser-cooled bunched ion beams from the Schottky spectra is still a challenging task.

In summary, laser cooling of bunched relativistic $^{16}O^{5+}$ ion beams has been realized at the storage ring CSRe. To the best of our knowledge, Li-like $^{16}O^{5+}$ is the ion with the highest charge state, the highest transition energy, and the highest kinetic energy to be directly laser cooled. It is demonstrated that the initially injected and bunched ion beams have been laser cooled using a continuous-wave (cw), single-mode narrow-linewidth diode laser system. With laser cooling, the relative longitudinal momentum spread of O^{5+} ion beams reached $\Delta p/p \approx 2.0 \times 10^{-6}$, which is one order of magnitude smaller than what can be reached using electron cooling [46]. In addition, the longitudinal Schottky spectra of laser-cooled bunched ion beams were simulated using our multiparticle phase-space tracking method, providing valuable insights into the experimental observations. Furthermore, the insights gained are expected to serve as a valuable reference for the laser cooling of extremely relativistic ion beams and the corresponding generation of high-intensity beams of

gamma rays, which have been proposed at the SPS and the LHC to, e.g., investigate atomic structure and test fundamental symmetries [47–49].

Appendix: Methods and derivations. Laser cooling of bunched ion beams, as first demonstrated in the ASTRID storage ring [13], utilizes the restoring force of the bucket to counteract the laser force. The phase-space diagrams are shown in Fig. 5 for the motion of a single ion under laser cooling in an rf bucket [7,21,37].

For this cooling scheme, only one cw laser counterpropagating to the ion beam is needed to provide a momentum-dependent friction force which damps the synchrotron oscillation of the ions in the bucket to realize laser cooling. The laser force:

$$F_{\text{laser}} = \frac{\hbar S k_{\text{laser}} (\Gamma/2)^3}{[\omega_{\text{laser}} \gamma (1+\beta) - \omega_0 (1+\beta) + k_0 v_i]^2 + (1+S)(\Gamma/2)^2},$$
(A1)

where $\hbar$ is the reduced Planck's constant, S the on-resonance saturation parameter, k_{laser} the wave number of the laser, Γ the natural linewidth of the transition, ω_{laser} the laser frequency, β and γ the relativistic factors of the resonant ions with the laser, ω_0 the transition frequency, k_0 the wave number of the transition, and v_i the velocity of the calculated ions.

A sinusoidal voltage is applied to the rf buncher, which is composed of two exciter plates with length of 25 cm, to

FIG. 5. Phase-space diagram for laser cooling of a single ion in an rf bucket. The trajectory of the ion, velocity-dependent deceleration laser force, as well as the position-dependent restoring bucket force, are shown.

longitudinally bunch the ion beams at the storage ring. In the comoving frame, it exerts a position-dependent force when the bunching frequency tuned to a harmonic number h of the revolution frequency f_{rev}. Ions that do not exactly match the synchronous velocity will perform synchrotron oscillations in the rf bucket, and the corresponding bucket force:

$$F_{\text{rf}}(z) = \frac{qeU_b}{C} \sin\left(\frac{2\pi h z}{C}\right),$$
(A2)

where qe is the ion charge, U_b bunching voltage, h harmonic number, and C circumference of the storage ring.

The longitudinal dynamics of laser-cooled bunched ion beams were investigated by observing the Schottky signals in real time with a high-sensitivity Schottky resonator. An image charge will be induced when a single ion passes through a Schottky resonator in the storage ring, and the induced beam current for a single bunched ion in the time domain is

$$i(t) = qef_{\text{rev}} \sum_{n=0}^{\infty} \delta[t - nt_{\text{rev}} - \tau \sin(2\pi f_{\text{syn}} t + \psi)], \quad (A3)$$

where qe is the ion charge, f_{rev} the revolution frequency, t_{rev} the revolution period, δ the Dirac delta function, n the revolution index, τ the oscillation time amplitude of the synchrotron motion, f_{syn} the synchrotron oscillation frequency, and ψ the initial phase of the ion. By using the Bessel series expansion, Eq. (A3) can be written as

$$
\begin{aligned}
i(t) = qef_{\text{rev}} + 2qef_{\text{rev}} \sum_{n=1}^{\infty} \sum_{p=-\infty}^{\infty} J_p(2\pi n f_{\text{rev}} \tau) \\
\times \cos[2\pi(n f_{\text{rev}} + p f_{\text{syn}})t + p\psi],
\end{aligned}
$$
(A4)

where p is the Bessel order and J_p is the Bessel function of order p. By Fourier transform, the beam current in the frequency domain is

$$i(f) = 2qef_{\text{rev}} \sum_{n=1}^{\infty} \sum_{p=-\infty}^{\infty} J_p(2\pi n f_{\text{rev}} \tau) \delta(f - (n f_{\text{rev}} + p f_{\text{syn}})).$$
(A5)

Therefore, the longitudinal Schottky signal for each observation frequency $(n f_{\text{rev}})$ is composed of an infinite number of synchrotron satellites spaced by the synchrotron frequency f_{syn}, while the amplitude of each satellite is proportional to the square of the Bessel coefficient $[J_p^2(2\pi n f_{\text{rev}} \tau)]$ since the Schottky power is proportional to the square of the signal amplitude $(P \propto i^2)$. As a result, the Schottky spectra of bunched ion beams, as shown in Fig. 3, are composed of a central peak and a series of symmetric and equidistant sidebands. It should be noted that only a moderate bunching voltages of a few volts in the present experiment result in a weak axial confinement of the ions and thus the synchrotron frequency of f_{syn} ($\sim$219 Hz) is orders of magnitude smaller than the betatron frequency ($\sim$3.5 MHz) at the CSRe.

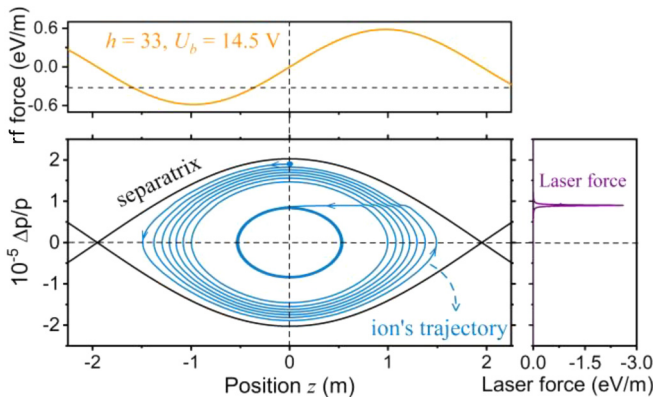Finally, the rms method was used to extract the momentum spread from the Schottky spectra of the laser-cooled bunched

O^{5+} ion beams. The first step of the rms method is to calculate the rms width of the sidebands of the Schottky spectrum:

$$\sigma_f^2 = \int_{-\infty}^{\infty} W(f)(f - f_0)^2 df, \qquad (A6)$$

where $W(f_i) = P(f_i)/\sum_{i=1}^{N} P(f_i)$ is the normalized Schottky power distributions in frequency, $P(f_i)$ the Schottky power with frequency f_i, and f_0 the frequency of the central peak. Then, one can calculate the rms width of the momentum spread with the Schottky spectrum:

$$\sigma_p/p = \eta^{-1} \times \sigma_f/f, \qquad (A7)$$

where η is the phase slip factor. Besides, rms width of the momentum spread can be calculated by ion distribution:

$$\sigma_p^2 = \int_{-\infty}^{\infty} W(p)(p - p_0)^2 dp, \qquad (A8)$$

where $W(p_i) = N(p_i)/\sum_{i=1}^{N} N(p_i)$ is the normalized momentum distribution function of the ion beams, p_i the average momentum point, $N(p_i)$ the number of ions with momentum p_i, and p_0 the central momentum. It can be found from Fig. 3 and Fig. 4 that the longitudinal rms momentum spreads can be deduced from the width of the incoherent Schottky sideband distribution very well, however, a precise derivation of the very small $\Delta p/p$ of laser-cooled bunched ion beams from the Schottky spectra is still a challenging task and needs further investigation.

[1] L. Schmöger, O. O. Versolato, M. Schwarz, M. Kohnen, A. Windberger, B. Piest, S. Feuchtenbeiner, J. Pedregosa-Gutierrez, T. Leopold, P. Micke *et al.*, Science **347**, 1233 (2015).

[2] M. S. Safronova, D. Budker, D. DeMille, D. F. J. Kimball, A. Derevianko, and C. W. Clark, Rev. Mod. Phys. **90**, 025008 (2018).

[3] M. G. Kozlov, M. S. Safronova, J. R. C. López-Urrutia, and P. O. Schmidt, Rev. Mod. Phys. **90**, 045005 (2018).

[4] S. A. King, L. J. Spieß, P. Micke, A. Wilzewski, T. Leopold, J. R. C. López-Urrutia, and P. O. Schmidt, Phys. Rev. X **11**, 041049 (2021).

[5] S. A. King, L. J. Spieß, P. Micke, A. Wilzewski, T. Leopold, E. Benkler, R. Lange, N. Huntemann, A. Surzhykov, V. A. Yerokhin *et al.*, Nature (London) **611**, 43 (2022).

[6] D. Habs and R. Grimm, Annu. Rev. Nucl. Part. Sci. **45**, 391 (1995).

[7] U. Schramm and D. Habs, Prog. Part. Nucl. Phys. **53**, 583 (2004).

[8] T. Schatz, U. Schramm, and D. Habs, Nature (London) **412**, 717 (2001).

[9] M. Nakao, T. Hiromasa, H. Souda, M. Tanabe, T. Ishikawa, H. Tongu, A. Noda, K. Jimbo, T. Shirai, M. Grieser *et al.*, Phys. Rev. ST Accel. Beams **15**, 110102 (2012).

[10] M. Steck and Y. A. Litvinov, Prog. Part. Nucl. Phys. **115**, 103811 (2020).

[11] S. Schröder, R. Klein, N. Boos, M. Gerhard, R. Grieser, G. Huber, A. Karafillidis, M. Krieg, N. Schmidt, T. Kühl *et al.*, Phys. Rev. Lett. **64**, 2901 (1990).

[12] J. S. Hangst, M. Kristensen, J. S. Nielsen, O. Poulsen, J. P. Schiffer, and P. Shi, Phys. Rev. Lett. **67**, 1238 (1991).

[13] J. S. Hangst, J. S. Nielsen, O. Poulsen, P. Shi, and J. P. Schiffer, Phys. Rev. Lett. **74**, 4432 (1995).

[14] H. J. Miesner, M. Grieser, R. Grimm, I. Lauer, V. Luger, P. Merz, A. Peters, U. Schramm, D. Schwalm, and M. Stößel, Nucl. Instrum. Methods Phys. Res. Sect A **383**, 634 (1996).

[15] U. Schramm, M. Bussmann, D. Habs, T. Kuhl, P. Beller, B. Franzke, F. Nolden, M. Steck, G. Saathoff, S. Reinhardt *et al.*, AIP Conf. Proc. **821**, 501 (2006).

[16] O. Boine-Frankenheim and T. Shukla, Phys. Rev. ST Accel. Beams **8**, 034201 (2005).

[17] R. W. Hasse, Phys. Rev. Lett. **86**, 3028 (2001).

[18] M. Bussmann, D. Habs, U. Schramm, K. Beckert, P. Beller, B. Franzke, W. Nörtershäuser, F. Nolden, M. Steck, S. Karpuk *et al.*, in *Proceedings of the Workshop on Beam Cooling and Related Topics, COOL07* (Bad Kreuznach, Germany, 2007), pp. 226–229.

[19] M. Bussmann, U. Schramm, D. Habs, M. Steck, T. Kühl, K. Beckert, P. Beller, B. Franzke, W. Nörtershäuser, C. Geppert *et al.*, J. Phys.: Conf. Ser. **88**, 012043 (2007).

[20] U. Schramm, M. Bussmann, and D. Habs, Nucl. Instrum. Methods. Phys. Res. Sect. A. **532**, 348 (2004).

[21] M. Bussmann, ICFA Beam Dyn. Newsletter **65**, 8 (2014).

[22] M. W. Bruker, S. Benson, A. Hutton, K. Jordan, T. Powers, R. Rimmer, T. Satogata, A. Sy, H. Wang, S. Wang *et al.*, Phys. Rev. Accel. Beams **24**, 012801 (2021).

[23] M. Blaskiewicz, J. M. Brennan, and K. Mernick, Phys. Rev. Lett. **105**, 094801 (2010).

[24] J. Ullmann, Z. Andelkovic, C. Brandau, A. Dax, W. Geithner, C. Geppert, C. Gorges, M. Hammen, V. Hannen, S. Kaufmann *et al.*, Nat. Commun. **8**, 15484 (2017).

[25] H. Backe, Hyperfine Interact. **171**, 93 (2006).

[26] X. Ma, W. Q. Wen, S. F. Zhang, D. Y. Yu, R. Cheng, J. Yang, Z. K. Huang, H. B. Wang, X. L. Zhu, X. Cai *et al.*, Nucl. Instrum. Methods Phys. Res. Sect. B **408**, 169 (2017).

[27] W. Wen, H. Wang, Z. Huang, D. Zhang, D. Chen, D. Winters, S. Klammes, D. Kiefer, T. Walther, S. Litvinov *et al.*, Hyperfine Interact. **240**, 45 (2019).

[28] T. Stöhlker, H. F. Beyer, H. Bräuning, A. Bräuning-Demian, C. Brandau, S. Hagmann, C. Kozhuharov, H. J. Kluge, T. Kühl, D. Liesen *et al.*, Nucl. Instrum. Methods Phys. Res. Sect. B **261**, 234 (2007).

[29] M. W. Krasny, arXiv:1511.07794.

[30] D. Budker, J. R. Crespo López-Urrutia, A. Derevianko, V. V. Flambaum, M. W. Krasny, A. Petrenko, S. Pustelny, A. Surzhykov, V. A. Yerokhin, and M. Zolotorev, Ann. Phys. **532**, 2000204 (2020).

[31] A. Martens, K. Cassou, R. Chiche, K. Dupraz, D. Nutarelli, Y. Peinaud, F. Zomer, Y. Dutheil, B. Goddard, M. W. Krasny *et al.*, Phys. Rev. Accel. Beams **25**, 101601 (2022).

[32] J. W. Xia, W. L. Zhan, B. W. Wei, Y. J. Yuan, M. T. Song, W. Z. Zhang, X. D. Yang, P. Yuan, D. Q. Gao, H. W. Zhao *et al.*, Nucl. Instrum. Methods Phys. Res. Sect. A **488**, 11 (2002).

[33] F. Nolden, P. Hülsmann, Y. A. Litvinov, P. Moritz, C. Peschke, P. Petri, M. S. Sanjari, M. Steck, H. Weick, J. X. Wu *et al.*, Nucl. Instrum. Methods Phys. Res. Sect. A **659**, 69 (2011).

[34] J. X. Wu, Y. D. Zang, F. Nolden, M. S. Sanjari, P. Hülsmann, F. Caspers, T. C. Zhao, M. Li, J. Z. Zhang, J. Li *et al.*, Nucl. Instrum. Methods Phys. Res. Sect. B **317**, 623 (2013).

[35] S. Chattopadhyay, AIP Conf. Proc. **127**, 467 (1985).

[36] D. Boussard, CERN Tech. Rep. No. CERN-SPS-86-11-ARF (1986).

[37] U. Schramm, T. Schätz, and D. Habs, Phys. Rev. Lett. **87**, 184801 (2001).

[38] W. Q. Wen, X. Ma, M. Bussmann, Y. J. Yuan, D. C. Zhang, D. F. A. Winters, X. L. Zhu, J. Li, H. P. Liu, D. M. Zhao *et al.*, Nucl. Instrum. Methods Phys. Res. Sect. A **736**, 75 (2014).

[39] H. B. Wang, D. Y. Chen, Y. J. Yuan, W. Q. Wen, Z. K. Huang, D. C. Zhang, D. Winters, S. Klammes, D. Kiefer, T. Walther *et al.* (unpublished).

[40] D. Y. Chen, H. B. Wang, W. Q. Wen, Y. J. Yuan, D. C. Zhang, Z. K. Huang, D. Winters, S. Klammes, D. Kiefer, T. Walther *et al.*, Nucl. Instrum. Methods Phys. Res. Sect. A **1047**, 167852 (2023).

[41] K. Lasocha and D. Alves, Phys. Rev. Accel. Beams **23**, 062803 (2020).

[42] V. Balbekov and S. Nagaitsev, in Proc. EPAC'042004, p. 791.

[43] M. Bussmann, U. Schramm, and D. Habs, AIP Conf. Proc. **862**, 221 (2006).

[44] M. Bussmann, U. Schramm, P. Thirolf, and D. Habs, in *High Performance Computing in Science and Engineering, Garching/Munich (2009)*, edited by S. Wagner, M. Steinmetz, A. Bode, and M. M. Müller (Springer, Berlin, Heidelberg, 2010), p. 589.

[45] N. Madsen, P. Bowe, M. Drewsen, L. H. Hornekær, N. Kjærgaard, A. Labrador, J. S. Nielsen, J. P. Schiffer, P. Shi, and J. S. Hangst, Phys. Rev. Lett. **83**, 4301 (1999).

[46] H. Zhao, L. Mao, J. Yang, J. Xia, X. Yang, J. Li, M. Tang, G. Shen, X. Ma, B. Wu *et al.*, Phys. Rev. Accel. Beams **21**, 023501 (2018).

[47] D. Budker, M. Gorchtein, M. W. Krasny, A. Pálffy, and A. Surzhykov, Ann. Phys. **534**, 2200004 (2022).

[48] J. Bieroń, M. W. Krasny, W. Płaczek, and S. Pustelny, Ann. Phys. **534**, 2100250 (2022).

[49] M. W. Krasny, A. Petrenko, and W. Płaczek, Prog. Part. Nucl. Phys. **114**, 103792 (2020).